

# Homoaromaticity in Tris(ethylene)nickel(0) and Tris(ethyne)nickel(0)

Rainer Herges\* and Andrea Papafilippopoulos

Since Wilke et al. synthesized tris(ethylene)nickel(0) (**1**) in 1973,<sup>[1]</sup> the structure of this first binary metal ethylene complex<sup>[2]</sup> and other nickel(0) alkene and alkyne complexes<sup>[3]</sup> have been thoroughly investigated. A major motivation of interest in these structures is the fact that Ni<sup>0</sup> complexes catalyze the synthetically and industrially important cyclo-oligomerization of alkenes and alkynes.<sup>[4, 5]</sup> A number of comprehensive studies notwithstanding,<sup>[6]</sup> we are still far from understanding all mechanistic details of these reactions.

There are two conceivable trigonally coordinated, highly symmetrical structures of tris(ethylene)nickel(0), one with the Ni atom and all carbon atoms in a plane (**1a**) and the other with the double bonds perpendicular to the coordination plane (**1b**; see Figure 1). These have been termed “planar” (**1a**) and “upright” (**1b**) by Hoffmann and Rösch.<sup>[7]</sup> Even though Wilke et al. suggested the correct structure **1a** immediately after synthesis, it is by no means trivial to explain the preference of the “planar” structure. Pitzer and Schaefer III predicted by ab initio calculations that the planar structure is 24 kcal mol<sup>-1</sup> more stable than the the upright conformer.<sup>[8]</sup> According to Hoffmann and Rösch the stabilization of **1a** is due to a more efficient interaction of the  $\pi^*$  MOs of the ethylene units with the 3d orbitals of Ni.<sup>[7]</sup> Pitzer and Schaefer III basically agree with this interpretation.<sup>[8]</sup> The corresponding parent tris(ethyne)nickel(0) complex (**2**) is not known but planar derivatives were synthesized by Youngs et al.<sup>[9]</sup> The parent compound **2** is expected not to be completely flat, because of the steric interaction of the acetylene hydrogen atoms.<sup>[10]</sup>

We have now found a surprisingly strong cyclic homoconjugation between the ethylene units in the planar structure **1a** and between the ethyne ligands in the *D*<sub>3</sub> structure of tris(ethyne)nickel(0) (**2a**). The C...C distance between the ligands of 2.681 Å in **1a** and 2.703 Å in **2a**<sup>[11]</sup> is in each case far below the sum of the van der Waals radii of the neighboring sp<sup>2</sup> and sp carbon atoms. Thus, **1a** and **2a** can be designated to be aromatic or “on the way” to trimerizing to cyclohexane and benzene, respectively. This does not only explain the preference of the planar arrangement of the fragments in **1** but also sheds light upon the role of nickel(0) as a catalyst in C–C bond formation processes.

Our results among other methods are based on a recently published method for the investigation of delocalization and conjugation effects in molecules.<sup>[12]</sup> This ACID (anisotropy of the induced current density) method provides a powerful and general way to visualize the density of delocalized electrons and to quantify conjugation effects. We have shown that the ACID scalar field can be interpreted as the density of

delocalized electrons. Even subtle effects such as the homoconjugation in cycloheptatriene and the anomeric effect are clearly visible in the corresponding ACID plots.<sup>[12]</sup>

Figure 1 presents the ACID plots<sup>[12]</sup> of planar **1a**, and upright-tris(ethylene)nickel(0) (**1b**) and *D*<sub>3</sub>-tris(ethyne)nickel(0) (**2a**).<sup>[13]</sup> There is a strong interaction between the central nickel atom and the three ethylene units in the planar structure **1a**. Coordination is much weaker (only visible at lower isosurface values) in upright **1b**. Most interesting, and surprising, however, is the strong cyclic homoconjugation between the three ethylene ligands. We defined the critical isosurface value (CIV) (the lowest ACID value in space between two interacting units) as a measure of the strength of a conjugation.<sup>[12]</sup> With a CIV of 0.0639 between the ethylene ligands in the planar complex **1a**, this value is in the range of the aromatic transition state of the parent Diels–Alder reaction<sup>[14]</sup> (0.0686) and only 0.01 lower than the CIV describing the  $\pi$  conjugation in benzene (0.0739). The interaction of the three ethylene units without Ni but fixed in the same geometry as in the planar complex is considerably smaller (CIV = 0.0263), indicating a very weak homoconjugation in the absence of nickel (Figure 1). The ACID value at a naked nickel atom without ligands is exactly zero. Hence, the homoaromaticity arises from the interaction of the three ethylene units with the central nickel atom.

Remaining doubts on an homoaromatic interaction of the three ethylene units in **1a** and **2a** can be eliminated by plotting the current density vectors onto the ACID isosurface (Figure 2). The current density vectors indicate a strong diamagnetic ring current<sup>[15]</sup> in the periphery which is typical for an aromatic system.<sup>[16]</sup>

Other magnetic parameters as well point to a considerable degree of aromaticity<sup>[17]</sup> in **1a** and **2a** (see Table 1). The magnetic susceptibility  $\chi$  and more importantly the anisotropy of the magnetic susceptibility  $\Delta\chi$  have been used as a measure for aromaticity.<sup>[18]</sup> Both  $\chi$  and  $\Delta\chi$  are more negative in aromatic compounds than in nonaromatic reference structures. For example  $\chi$  for benzene and fulvene is –46.1 and –34.1 ppm (cgs), respectively; the corresponding values for  $\Delta\chi$  are –69.7 and –34.2.<sup>[13]</sup> A similar trend is found in **1a** and **1b** and in **2a** and **2b**. The planar structures exhibit considerably more negative values for  $\chi$  and  $\Delta\chi$  (Table 1). The size of the effect is typical for aromatic compounds.<sup>[18]</sup> According to the  $\Delta\chi$  values the aromaticity is somewhat less pronounced in **2a** than in **1a**. This might be due to the nonplanar conformation and the resulting less efficient interaction of the acetylene ligands. The large positive value of  $\Delta\chi$  in **2b** arises from the anisotropy of the acetylene ligands.

If there is a ring current in **1a** and **2a**, the nickel atoms should exhibit a large upfield NMR shift compared to the nonaromatic counterparts **1b** and **2b** because the nickel atoms are exactly placed in the center of the ring where the shielding induced by the ring current is largest. This is indeed the case. The calculated upfield shift in **1a** versus **1b** is extraordinarily large and amounts to 1847.7 ppm and to 1826.9 ppm in **2a** versus **2b**.<sup>[13, 19]</sup> Again the aromaticity in **2a** obviously is somewhat lower than that in **1a** (Table 1).

What is the origin of this remarkable homoaromaticity in **1a** and **2a**? A simple and straightforward answer is provided

[\*] Prof. Dr. R. Herges, A. Papafilippopoulos  
Institut für Organische Chemie  
Universität Kiel  
Otto Hahn-Platz 4, 24098 Kiel (Germany)  
Fax: (+49) 431-880-1558  
E-mail: rherges@oc.uni-kiel.de

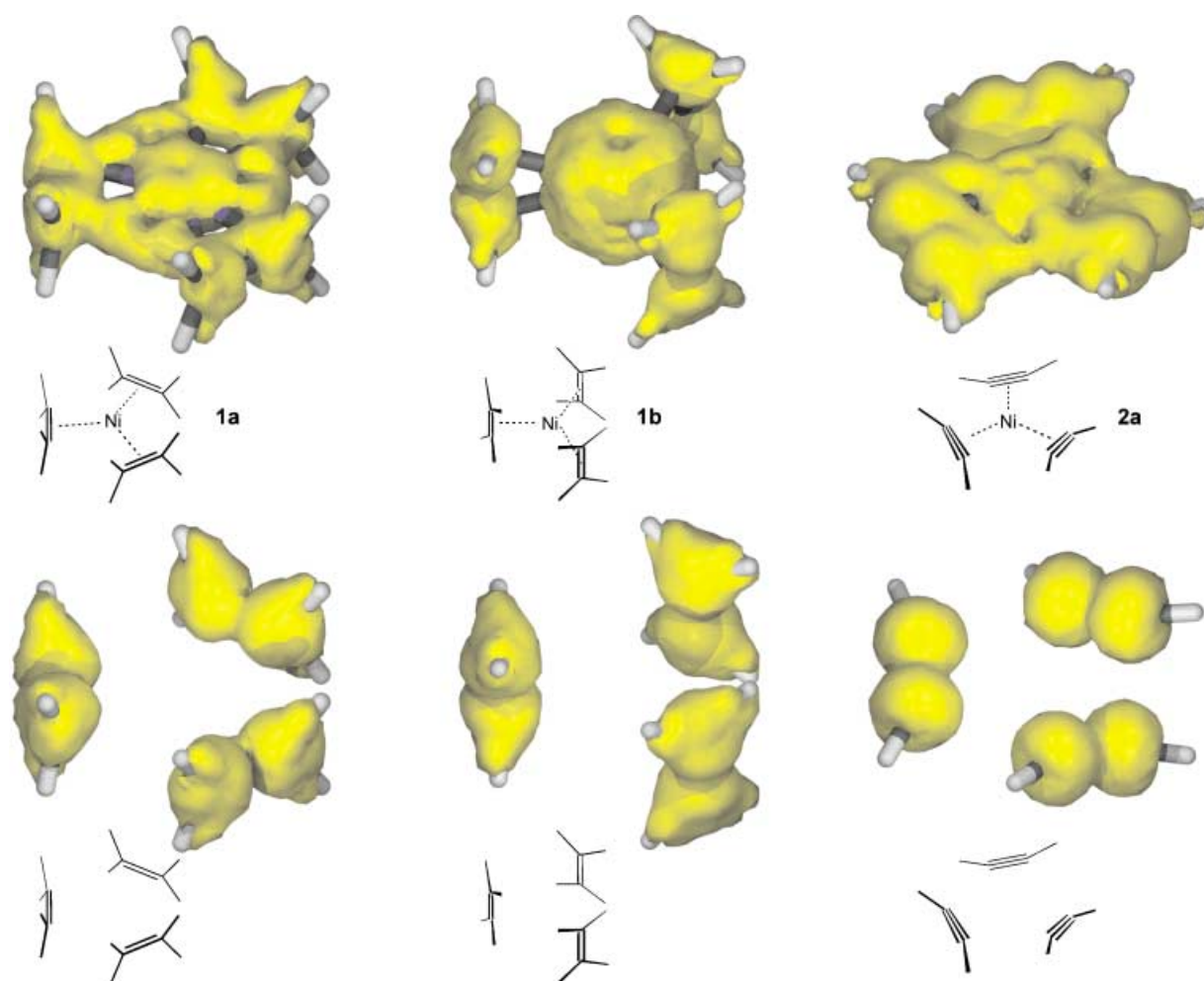


Figure 1. Delocalized electrons in planar and upright-tris(ethylene)nickel(0) (**1a** and **1b**, respectively) and  $D_3$ -symmetrical tris(ethyne)nickel(0) (**2a** (first row)).<sup>[11]</sup> Delocalization in the nickel complexes is compared to conjugation in the free ligands without nickel (second row). The ligands are fixed in the geometry of the complexes. The isosurfaces are plotted using the ACID method<sup>[12]</sup> at an isosurface value of 0.05. Nickel atoms without ligands exhibit zero ACID (see text).

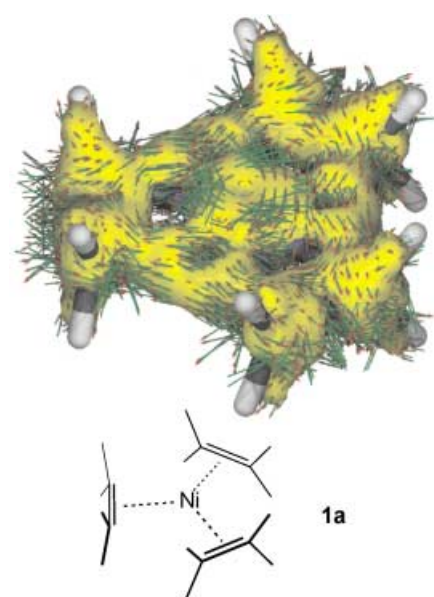


Figure 2. Current density vectors plotted onto the ACID surface of **1a**. The vector of the magnetic field is perpendicular to the coordination plane and pointing upwards.

Table 1. Calculated energies, imaginary frequencies (B3LYP/6-31 + G\*) and magnetic properties (CSGT) of planar and upright-tris(ethylene)nickel(0) (**1a** and **1b**, respectively) and  $D_3$ - and upright-tris(ethyne)nickel(0) (**2a** and **2b**, respectively).

	<b>1a</b> ( $D_{3h}$ )	<b>1b</b> ( $D_{3h}$ )	<b>2a</b> ( $D_3$ )	<b>2b</b> ( $D_{3h}$ )
$E_{\text{abs}}^{\text{[a]}}$	−1743.867904	−1743.822389	−1740.170096	−1740.104356
$E_{\text{rel}}^{\text{[b]}}$	0.0	28.4	0.0	41.3
$N_{\text{imag}}^{\text{[c]}}$	0	4	0	9
$\chi^{\text{[d]}}$	−82.5	−26.9	−65.1	+2.11
$\Delta\chi^{\text{[e]}}$	−56.5	−29.1	−47.5	+85.7
$\text{CIV}^{\text{[f]}}$	0.0639	0.0263	0.0565	−[g]
$\delta(^{61}\text{Ni})^{\text{[h]}}$	−1460.7	+387.0	−62.7	+1764.2

[a] In a.u. [b] Relative to the planar structures **1a** and **2a** in kcal mol<sup>−1</sup>. [c] Number of imaginary frequencies, according to a harmonic frequency calculation. [d] Magnetic susceptibility calculated using the CSGT method<sup>[20]</sup> in ppm (cgs). [e] Anisotropy of the magnetic susceptibility calculated from the magnetic susceptibility tensor according to  $\Delta\chi = \chi_{zz} - \chi_{xx}$ ,  $\chi_{zz}$  is the susceptibility component perpendicular to the ring plane,  $\chi_{xx}$  and  $\chi_{yy}$  are identical since **1a,b** and **2a,b** are symmetric tops (molecules with  $C_n$ ,  $n > 2$ ), the ring plane (xy) is defined by the midpoints of the C–C bonds and the Ni atom. [f] Critical isosurface value between the ligands (see text). [g] Topology of the ACID isosurface representing direct ligand–ligand interaction does not exist. [h] Ni NMR chemical shift relative to that of [Ni(CO)<sub>4</sub>], which is the generally accepted standard in <sup>61</sup>Ni NMR spectroscopy.

by qualitative MO theory. Hoffmann and Rösch already pointed out that there is an interaction of the  $\pi^*$  orbitals of the ethylene ligands with the 3d orbitals of nickel which is more efficient in the planar structure **1a** than in the upright conformer **1b**.<sup>[7]</sup> More specifically: in **1a** both, the  $\pi$  and  $\pi^*$  degenerate set of ethylene orbitals ( $e'$ ) interact with  $3d_{xy}$  and  $3d_{x^2-y^2}$  ( $e'$ ) of nickel (Figure 3). Mixing ethylene  $\pi^*$  character

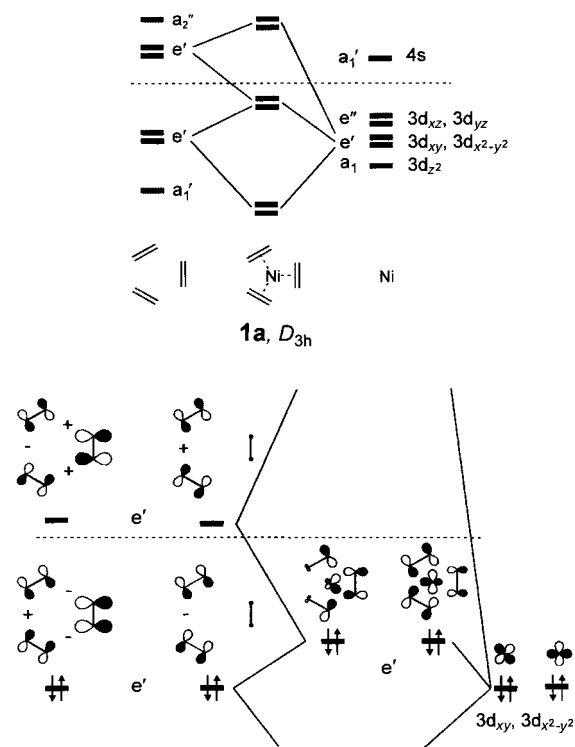


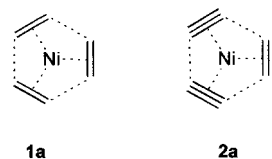
Figure 3. MO diagram for **1a** (top). Only the  $e'$  orbital interaction is shown. The detail from the MO diagram (bottom) illustrates the mixing of  $\pi$  and  $\pi^*$  orbitals of ethylene into the bonding orbitals of the complex. The coefficients of the  $D_{3h}$ -symmetry-adapted MOs of the ethylene  $\pi$  and  $\pi^*$  orbitals correspond to the ethylene units being at an infinite distance. The coefficients of the nickel complex are drawn using the Kohn–Sham orbitals of the density functional theory (DFT) calculation (see text). + signs denote bonding and – signs antibonding character between the ethylene units.

into the bonding orbitals of the complex lowers the bond order of the ethylene double bonds and increases bonding between the ethylene units leading to homoconjugation. Note that the  $e'$  orbital of the  $D_{3h}$ -symmetry-adapted orbitals of the  $\pi^*$  ethylene units (LUMO, Figure 3, left) has an overall ethylene–ethylene bonding character (two bonding, one antibonding interaction in the left orbital, one bonding interaction in the right orbital of the degenerate set), whereas the  $\pi$  ethylene orbitals (HOMO, Figure 3, left) are ethylene–ethylene antibonding (two antibonding and one bonding interaction in the left  $e'$  orbital and one antibonding interaction in the right  $e'$  orbital). The same is true for the tris(ethyne)nickel complex (**2**).

Thus the central nickel atom not only holds the three  $\pi$  ligands ethylene and ethyne in a favorable position for a trimerization ( $a_1'$  orbital interaction, see Figure 3) but also favors the reaction by lowering the  $\pi$  bond order within the

ligands and by increasing the bond order between the ligands. For completion of the hypothetical trimerization of ethylene to cyclohexane and the known reaction of ethyne to benzene, the nickel atom has to leave the center of the complex. A concerted cycloaddition process, the strong homoaromaticity notwithstanding, thus is unlikely and was not found by an extensive search on the reaction hypersurface. The mechanism in detail, probably is more complicated<sup>[5c, 6b–f, 21]</sup> and will be subject of further theoretical studies.

To depict the strong homoconjugation, the structural formula of **1a** and **2a** should be written with dashed lines connecting the ligands.



Received: May 28, 2001  
Revised: July 27, 2001 [Z17190]

- [1] K. Fischer, K. Jonas, G. Wilke, *Angew. Chem.* **1973**, *85*, 620–621; *Angew. Chem. Int. Ed. Engl.* **1973**, *12*, 565–566.
- [2] a) T. Merle-Mejean, C. Cosse-Mertens, S. G. F. Bouchareb, J. Mascetti, M. Tranquille, *J. Phys. Chem.* **1992**, *96*, 9148–9158; b) J. Mink, M. Gal, P. L. Goggin, J. L. Spencer, *J. Mol. Struct.* **1986**, *142*, 467–472; c) P. Csaszar, P. L. Goggin, J. Mink, J. L. Spencer, *J. Organomet. Chem.* **1989**, *379*, 337–349; d) H. Huber, G. A. Ozin, W. J. Power, *J. Am. Chem. Soc.* **1976**, *98*, 6508–6511; G. A. Ozin, W. J. Power, T. H. Upton, W. A. Goddard, *J. Am. Chem. Soc.* **1978**, *100*, 4750–4760.
- [3] For review see: a) G. Wilke, *Angew. Chem.* **1988**, *100*, 190–211; *Angew. Chem. Int. Ed. Engl.* **1988**, *27*, 186–206; b) M. J. Chetcuti in *Comprehensive Organometallic Chemistry II*, Vol. 9 (Eds.: E. W. Abel, F. G. A. Stone, G. Wilkinson), Elsevier Science, Oxford, **1994**, pp. 107–191.
- [4] The first nickel-catalyzed alkene and alkyne trimerizations were observed by Reppe: W. Reppe, W. J. Schueckendieck, *Liebigs Ann. Chem.* **1948**, 560, 104.
- [5] For review see: a) M. Lautens, W. Klute, *Chem. Rev.* **1996**, *96*, 49–92; b) N. E. Schore, *Chem. Rev.* **1988**, *88*, 1081–1119; c) P. W. Jolly in *Comprehensive Organometallic Chemistry*, Vol. 8 (Ed.: G. Wilkinson), Elsevier Science, Oxford, **1982**, pp. 649–670; d) W. Keim, A. Behr, M. Röper, *Comprehensive Organometallic Chemistry*, Vol. 8 (Ed.: G. Wilkinson), Elsevier Science, Oxford, **1982**, pp. 371–462; P. W. Jolly in *Comprehensive Organometallic Chemistry*, Vol. 8 (Ed.: G. Wilkinson), Elsevier Science, Oxford, **1982**, pp. 613–647.
- [6] a) U. Rosenthal, W. Schulz, *J. Organomet. Chem.* **1987**, *321*, 103–117; b) J. J. Eisch, J. E. Galle, *J. Organomet. Chem.* **1975**, *96*, C23–C26; c) H. Hoberg, W. Richter, *J. Organomet. Chem.* **1980**, *195*, 355–362; d) J. J. Eisch, J. E. Galle, A. A. Aradi, M. P. Boleslawski, *J. Organomet. Chem.* **1986**, *312*, 399–416; e) R. Diercks, L. Stamp, J. Kopf, H. Tom Dieck, *Angew. Chem.* **1984**, *96*, 891–895; *Angew. Chem. Int. Ed. Engl.* **1984**, *23*, 893–894; f) A. W. Parkins, R. C. Slade, *J. Chem. Soc. Dalton Trans.* **1975**, 1352–1356; g) K. Kitaura, S. Sakaki, K. Morokuma, *Inorg. Chem.* **1981**, *20*, 2292–2297; h) T. Ziegler, *Inorg. Chem.* **1985**, *24*, 1547–1552.
- [7] N. Rösch, R. Hoffmann, *Inorg. Chem.* **1974**, *13*, 2656–2666.
- [8] R. M. Pitzer, H. F. Schaefer III, *J. Am. Chem. Soc.* **1979**, *101*, 7176–7183.
- [9] a) J. D. Ferrara, C. Tessier-Youngs, W. J. Youngs, *J. Am. Chem. Soc.* **1985**, *107*, 6719–6721; b) J. D. Ferrara, A. A. Tanaka, C. Fierro, C. A. Tessier-Youngs, W. J. Youngs, *Organometallics* **1989**, *8*, 2089–2098; c) W. J. Youngs, J. D. Kinder, J. D. Bradshaw, C. A. Tessier, *Organometallics* **1993**, *12*, 2406–2407.
- [10] G. A. Ozin, D. F. McIntosh, W. J. Power, R. P. Messmer, *Inorg. Chem.* **1981**, *20*, 1782–1792.
- [11] Selected distances [Å] and angles [°] (B3LYP/6-31 + G\*): **1a**: Ni–C 2.068, C–C 1.386, C–H 1.088, C···C 2.681, H–C–C 120.6, H–C–H 115.3; **1b**: Ni–C 2.165, C–C 1.369, C–H 1.089, C···C 3.557, H–C–C 121.3, H–C–H 116.1; **2a**: Ni–C 1.998, C–C 1.249, C–H 1.0737, H···H 2.614, C···C

- 2.703, H-C-C 155.85, the acetylene units are twisted by 15° out of the hypothetical coordination plane.
- [12] R. Herges, D. Geuenich, *J. Phys. Chem. A* **2001**, *105*, 3214–3220.
- [13] The structures were optimized and checked by harmonic frequency analysis at the B3LYP/6-31 + G\* level of theory using the Gaussian 98 suite of programs. Chemical shifts and magnetic susceptibilities are calculated at the same level of theory using the CSGT method implemented in Gaussian 98 (Revision A.7), M. J. Frisch, G. W. Trucks, H. B. Schlegel, G. E. Scuseria, M. A. Robb, J. R. Cheeseman, V. G. Zakrzewski, J. A. Montgomery, R. E. Stratmann, J. C. Burant, S. Dapprich, J. M. Millam, A. D. Daniels, K. N. Kudin, M. C. Strain, O. Farkas, J. Tomasi, V. Barone, M. Cossi, R. Cammi, B. Mennucci, C. Pomelli, C. Adamo, S. Clifford, J. Ochterski, G. A. Petersson, P. Y. Ayala, Q. Cui, K. Morokuma, D. K. Malick, A. D. Rabuck, K. Raghavachari, J. B. Foresman, J. Cioslowski, J. V. Ortiz, B. B. Stefanov, G. Liu, A. Liashenko, P. Piskorz, I. Komaromi, R. Gomperts, R. L. Martin, D. J. Fox, T. Keith, M. A. Al-Laham, C. Y. Peng, A. Nanayakkara, C. Gonzalez, M. Challacombe, P. M. W. Gill, B. G. Johnson, W. Chen, M. W. Wong, J. L. Andres, M. Head-Gordon, E. S. Replogle, J. A. Pople, Gaussian, Inc., Pittsburgh, PA, **1998**.
- [14] R. Herges, H. Jiao, P. von R. Schleyer, *Angew. Chem.* **1994**, *106*, 1441; *Angew. Chem. Int. Ed. Engl.* **1994**, *33*, 1376–1378.
- [15] For a very thorough review on the concept of the ring current see: P. Lazzaretti, *Prog. Nucl. Magn. Reson. Spectrosc.* **2000**, *36*, 1–88.
- [16] For a very recent application of current density plots on coronene and corannulene see: E. Steiner, P. W. Fowler, L. W. Jenneskens, *Angew. Chem.* **2001**, *113*, 375–379; *Angew. Chem. Int. Ed.* **2001**, *113*, 362–366.
- [17] P. von R. Schleyer, H. Jiao, *Pure Appl. Chem.* **1996**, *68*, 209–218.
- [18] W. H. Flygare, *Chem. Rev.* **1974**, *74*, 653.
- [19] Experimental <sup>61</sup>Ni NMR chemical shifts on tris(ethylene)nickel(0) unfortunately are not known. Because of its large quadrupole moment (0.16 × 10<sup>-28</sup> m<sup>2</sup>), low natural abundance (1.19%), and low receptivity the <sup>61</sup>Ni NMR chemical shifts of only two trigonal-planar Ni<sup>0</sup> complexes ([Ni(cdt)] (cdt = all-trans-1,5,9-cyclododecatriene) and [Ni(C<sub>2</sub>H<sub>4</sub>)<sub>2</sub>(PMe<sub>3</sub>)]]) have been published: a) R. Benn, A. Rufinska, *Angew. Chem.* **1986**, *98*, 851–871; *Angew. Chem. Int. Ed. Engl.* **1986**, *25*, 861–881. Further data on tetrahedral, zero-valent complexes: b) K. D. Behringer, J. Blümel, *Magn. Reson. Chem.* **1995**, *33*, 729–733; c) N. Hao, M. J. McGlinchey, B. G. Sayer, G. J. Schrobilgen, *J. Magn. Reson.* **1982**, *46*, 159–162; d) H. Schumann, M. Meißner, H.-J. Kroth, *Z. Naturforsch. B* **1980**, *35*, 639–641; e) R. Benn, A. Rufinska, *Magn. Reson. Chem.* **1988**, *26*, 895–902.
- [20] T. A. Keith, R. F. W. Bader, *J. Chem. Phys. A* **1993**, *99*, 3669–3693.
- [21] a) K.-R. Pörschke, *Angew. Chem.* **1987**, *99*, 1321–1322; *Angew. Chem. Int. Ed. Engl.* **1987**, *26*, 1288; b) K.-R. Pörschke, *J. Am. Chem. Soc.* **1989**, *111*, 5691–5699; c) T. Takahashi, F.-Y. Tsai, Y. Li, K. Nakajima, M. Kitora, *J. Am. Chem. Soc.* **1999**, *121*, 11093–11100.

## On the Stability of Electrochemically Generated Nanoclusters—A Computer Simulation\*\*

Mario G. Del Pópolo, Ezequiel P. M. Leiva,\* and Wolfgang Schmickler\*

The scanning tunneling microscope (STM), operated in an electrochemical environment, offers a precise and cheap way to produce small metal clusters on a foreign substrate. Pioneering work in this area has been performed by Kolb, Ullmann, and Will,<sup>[1]</sup> who developed the following procedure for the deposition of nanosized copper clusters on single-crystal gold electrodes: The gold electrode is held at a potential a little positive of the deposition potential for copper, while the tip potential is set below this value, so that copper atoms are deposited on the tip surface. The tip is then pressed against the electrode and withdrawn again. As the tip separates from the electrode a metal cluster remains, which typically comprises 20–100 atoms, and is a few monolayers high. This method also works for the generation of palladium clusters on Au(111), but not for copper on Ag(111).<sup>[1, 2]</sup>

The generation of such metal clusters is of great interest, since they are expected to play a major role in future nanotechnologies. The deposition of copper clusters on the Au(111) surface has been investigated most extensively, and is considered as a prototype for the electrochemical fabrication of nanoclusters. Recently, this process has attracted further attention because the copper clusters are stable at a potential at which bulk copper dissolves. This is surprising because generally clusters tend to be less stable than the corresponding bulk material. Kolb, Engelmann, and Ziegler<sup>[3]</sup> have speculated that this increased stability is caused by quantum confinement: They propose that the electrons in the cluster are separated from the bulk of the electrode by a potential energy barrier, so that the energy levels in the cluster are discrete and not continuous as in bulk metals. The dissolution

[\*] Prof. Dr. E. P. M. Leiva, M. G. Del Pópolo  
Universidad Nacional de Córdoba  
Unidad de Matemática y Física  
Facultad de Ciencias Químicas  
5000 Córdoba (Argentina)  
Fax: (+54) 351-4334189  
E-mail: eleiva@fcq.unc.edu.ar

Prof. Dr. W. Schmickler  
Abteilung Elektrochemie  
Universität Ulm  
89069 Ulm (Germany)  
Fax: (+49) 731-5025409  
E-mail: wolfgang.schmickler@chemie.uni-ulm.de

[\*\*] This work was supported by Consejo Nacional de Investigaciones Científicas y Técnicas (CONICET), by Consejo de Investigaciones Científicas y Tecnológicas de la Provincia de Córdoba (CONICOR), by the Secretaría de Ciencia y Técnica de la Universidad Nacional de Córdoba (SeCyT-UNC; program BID 802/OC-AR PICT Nr. 06-04505) and by the Fundación Antorchas (E.P.M.L and M.G.D.) as well as by the Deutsche Forschungsgemeinschaft under the program “Grundlagen der elektrochemischen Nanotechnologie” (W.S.). Some of the calculations were performed on a Digital workstation financed by the Alexander von Humboldt Stiftung.



Supporting information for this article is available on the WWW under <http://www.angewandte.com> or from the author.